Climate Dynamics manuscript No.
(will be inserted by the editor)

The effect of ocean mixed layer depth on climate in slab ocean aquaplanet experiments.

Aaron Donohoe · **Dargan Frierson**

Manuscript submitted January 17, 2013

ABSTRACT

The effect of ocean mixed layer depth on climate is explored in a suite of slab ocean aquaplanet simulations with different mixed layer depths.

Keywords seasonal cycle · aquaplanet · expansion of tropics

1. Introduction

The seasonal cycle of temperature in the extratropics is driven by seasonal variations in insolation that are comparable in magnitude to the annual mean insolation. The majority of the seasonal variations in insolation are absorbed in the ocean Fasullo and Trenberth (2008a,b), which has a much larger heat capacity than the overlying atmosphere; this energy never enters the atmospheric column to drive seasonal variations in atmospheric temperature and circulation. The heat capacity of the ocean plays a fundamental role in setting both the magnitude and phasing of the seasonal cycle in the atmosphere. The Earth's climate would be fundamentally different if the ocean's heat capacity was not substantially larger than that of the atmosphere.

Aaron Donohoe

Dept. of Earth, Atmospheric and Planetary Sciences, Room Number 54-918, 77 Massachusetts Avenue, Cambridge, MA 02139-4307. E-mail: thedhoe@mit.edu

D. Frierson

Department of Atmospheric Sciences, University of Washington, Seattle, Washington

In a forced system with a heat capacity and a linear, negative feedback (damping), the system response is in quadrature phase with the forcing if the heat capacity (times the angular forcing frequency) is much larger than the feedback parameter. In contrast, the system response is in phase with the forcing if the feedback parameter is substantially larger than the heat capacity. Therefore, in the extratropical climate system– where the insolation is the forcing and the Planck feedback and meridional atmospheric energy fluxes are the dominant negative feedbacks– one would expect that the phase lag of temperature with respect to insolation would increase with increasing ocean heat capacity. We will demonstrate that this expectation does not come true in an idealized set of experiments; the phase lag of atmospheric temperature is a non-monotonic function of ocean heat capacity. We argue that increasing ocean heat capacity moves the system from a regime in which the seasonal heating of the atmosphere is dominated by the energy fluxes from the surface (ocean) to the atmosphere to a regime where the heating is dominated by the sun heating the atmosphere directly via shortwave absorption in the atmospheric column. In the latter regime, the surface and atmospheric energy budgets are partially decoupled and the atmospheric heating is nearly in phase with the insolation resulting in a small phase lag of the seasonal temperature response. Recently, Donohoe and Battisti (2012) demonstrated that the seasonal heating of the atmosphere in the observations is dominated by direct shortwave absorption in the atmospheric column as a opposed to surface energy fluxes which is akin to the large ocean heat capacity regime discussed above.

The heat capacity of the climate system does not contribute to the annual mean energy budget in the theory of energy balance models (North 1975) because there is no heat storage in equilbruim. However, the magnitude of the seasonal cycle can impact the annual mean energy budget through the rectification of non-linearities and/or the covariance of processes acting over the seasonal cycle (i.e. the correlation between seasonal anomalies in insolation and albedo). Therefore, the ocean heat capacity may impact the annual mean climate of the. Indeed, we demonstrate here that the ocean heat capacity has a large impact on the modeled climate system in the annual mean including the global mean temperature, the global energy budget, the extent of the tropics, the meridional energy transport, and the location and intensity of the surface westerlies.

Slab ocean models are widely used to assess the equilibrium climate sensitivity global climate models (Danabasoglu and Gent 2009) because the system comes to equilibrium rapidly as compared to the full-depth ocean model. Slab ocean models are also widely used in idealized simulations (Kang et al. 2008; Rose and Ferreira 2013) to model the response of the climate system to prescribed anomalies in ocean heat transport. The sensitivity of climate to mixed layer depth in these simulations is often neglected.

In this study, we analyze the effect of slab ocean depth on climate (temperature, precipitation, winds, and energy fluxes) in a suite of aquaplanet slab ocean experiments, each with a different, globally uniform ocean mixed layer depth. This paper is organized as follows. In Section 2, we introduce the models and observational data sets we will compare the models to. We then analyze the amplitude and phase of the seasonal cycle of atmospheric temperature and interpret these results in terms of the source of the seasonal heating of the atmosphere. We then analyze the seasonal migration of the inter-tropical convergence zone (ITCZ) in the slab-ocean aquaplanet simulations and it's impact on the tropical precipitation (Section 3). We also demonstrate that the seasonal migration of the ITCZ has large impacts for the global mean planetary albedo and hence the global energy budget and global mean temperature in this section. Lastly, we demonstrate that the amplitude of seasonal cycle also modifies the meridional heat transport in the climate system by way of modifying the meridional structure of planetary albedo (Section 4). As a consequence, both the magnitude and location of the jets, including the surface westerlies, change as the amplitude of the seasonal cycle changes. A summary and discussion follows in Section 5.

2. Data

We will analyze the effect of ocean heat capacity on climate in a suite of slab-ocean aquaplanet simulations with different ocean mixed layer depths. Here we describe the model runs used. The analysis of the model output will be compared to observations to give the results context. We also describe the observational data sources in this section.

a. Slab-ocean aquaplanet simulations

An atmospheric general circulation is coupled to a slab ocean covering the entire globe with globally uniform mixed layer depth. Five ensemble members with prescribed ocean depths of 2.4, 6, 12, 24, and 50 meters are analyzed in this study. This range cover the case where the ocean has the same heat capacity as the atmospheric column to a case where the ocean heat capacity is approximately 20 times that of the atmosphere. There is no Q flux to the ocean; the ocean does not transport energy. The model integrations are preformed with the Geophysical Fluid Dynamics Lab

Atmospheric Model version 2.1 (Delworth et al. 2006) atmospheric model featuring a finite volume dynamical core (Lin 2004) with a horizontal resolution of approximately 2° latitude and 24 vertical levels. The model is forced by seasonally varying solar insolation with zero eccentricity and 23.439° obliquity, and is run for twenty years, sufficient to converge on a steady climatology. The model climatology is taken from the last five years of the integrations.

b. Observational data

We use the ERA interim analysis climatological (1979-2010) atmospheric temperature data to define the amplitude and phase of the observed atmospheric temperature.

The longwave and shortwave radiative fluxes at the TOA and the shortwave fluxes at the surface are from the Clouds and Earth's Radiant Energy System (CERES) experiment (Wielicki et al. 1996). We use the long term climatologies of the CERES TOA fluxes from Fasullo and Trenberth (2008a) that are corrected for missing data and global average energy imbalances. The surface shortwave radiation is taken from the CERES "AVG" fields that are derived by assimilating the satellite observations into a radiative transfer model to infer the surface radiative fluxes (Rutan et al. 2001). All calculations are preformed separately for each of the four CERES instruments (FM1 and FM2 on Terra from 2000 -2005 and FM3 and FM4 on AQUA from 2002 – 2005). We then average the results over the four instruments to compose monthly averaged climatologies over the observation period.

The atmospheric heat flux divergences are calculated using the velocity, temperature, specific humidity and geopotential fields from the ERA interim analysis. We use the 6 hourly instantaneous fields with a horizontal resolution of 1.5° and 37 vertical levels to calculate the atmospheric moist static energy fluxes using the advective form of the energy flux equations (Trenberth and Smith 2008) as discussed in the Appendix. This method satisfies the mass budget by construction and allows us to accurately calculate the energy flux divergences without explicitly balancing the mass budget with a barotropic wind correction. We note that, the calculated heat flux divergences are in close agreement with similar calculations by Fasullo and Trenberth (2008b) and the conclusions reached in this study do not depend on the dataset and methodology used to calculate the atmospheric energy fluxes. We calculate the vertical integral of the atmospheric energy tendency as follows: (1) the temperature and specific humidity tendency at each level is calculated as the centered finite difference of the monthly mean fields and (2) the mass integral is calculated as the weighted sum of the tendencies at each level multiplied by c_P and L respectively.

3. The amplitude and phase of the seasonal cycle of atmospheric temperature and the source of atmospheric heating

4. The seasonal migration of the ITCZ and it's impact on precipitation and global mean temperature

5. Meridional energy transport and jet location

Acknowledgements Place holder

REFERENCES

Danabasoglu, G. and P. Gent, 2009: Equilibrium climate sensitivity: is it accurate to use a slab ocean model? *J. Climate*, **22**, 2494–2499.

Delworth, T. L., A. J. Broccoli, A. Rosati, R. J. Stouffer, V. Balaji, J. A. Beesley, and W. F. Cooke, 2006: Gfdl's cm2 global coupled climate models. part i: Formulation and simulation characteristics. *J. Climate*, **19 (5)**, 643–674.

Donohoe, A. and D. Battisti, 2012: The seasonal cycle of atmospheric heating and temperature. in preparation.

Fasullo, J. T. and K. E. Trenberth, 2008a: The annual cycle of the energy budget: Part 1. global mean and land-ocean exchanges. *J. Climate*, **21**, 2297–2312.

Fasullo, J. T. and K. E. Trenberth, 2008b: The annual cycle of the energy budget: Part 2. meridional structures and poleward transports. *J. Climate*, **21**, 2313–2325.

Kang, S., I. Held, D. Frierson, and M. Zhao, 2008: The response of the itcz to extratropical thermal forcing: idealized slab-ocean experiments with a gcm. *J. Climate*, **21**, 3521–3532.

Lin, S. J., 2004: A "vertically lagrangian" finite-volume dynamical core for global models. *Mon. Weath. Rev.*, **132 (10)**, 2293–2307.

North, G. R., 1975: Theory of energy-balance climate models. *J. Atmos. Sci.*, **32**, 2033–2043.

Rose, B. and D. Ferreira, 2013: Ocean heat transport and water vapor greenhouse in a warm equable climate: a new look at the low gradient paradox. *J. Climate*, in press.

Rutan, D., F. Rose, N. Smith, and T. Charlock, 2001: Validation data set for CERES surface and atmospheric radiation budget (SARB). *WCRP/GEWEX Newsletter*, **11 (1)**, 11–12.

Trenberth, K. E. and L. Smith, 2008: Atmospheric energy budgets in the japanese reanalysis: Evaluation and variability. **86**, 579–592.

Wielicki, B., B. Barkstrom, E. Harrison, R. Lee, G. Smith, and J. Cooper, 1996: Clouds and the earth's radiant energy system (CERES): An earth observing system experiment. *Bull. Amer. Meteor. Soc.*, **77**, 853–868.

List of Figures

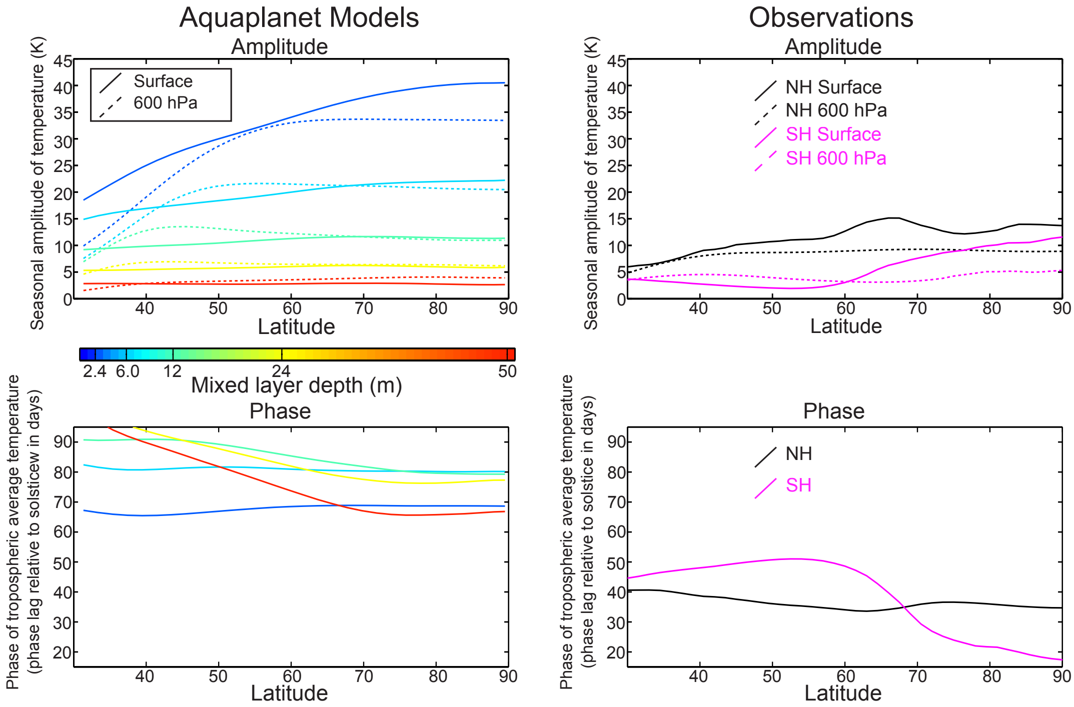

FIG. 1. (Top) The seasonal amplitude of atmospheric temperature at the surface (solid lines) and at 600 hPa (dashed lines) in the slab-ocean aquaplanet simulations (Left Panel) and observations (Right Panel). The different ocean mixed layer depths are indicated by the colorbar below the plot. (Bottom) Phase lag of seasonal cycle of atmospheric column integrated temperature with respect to insolation in the slab-ocean aquaplanet simulations (Left) and observations (Right).

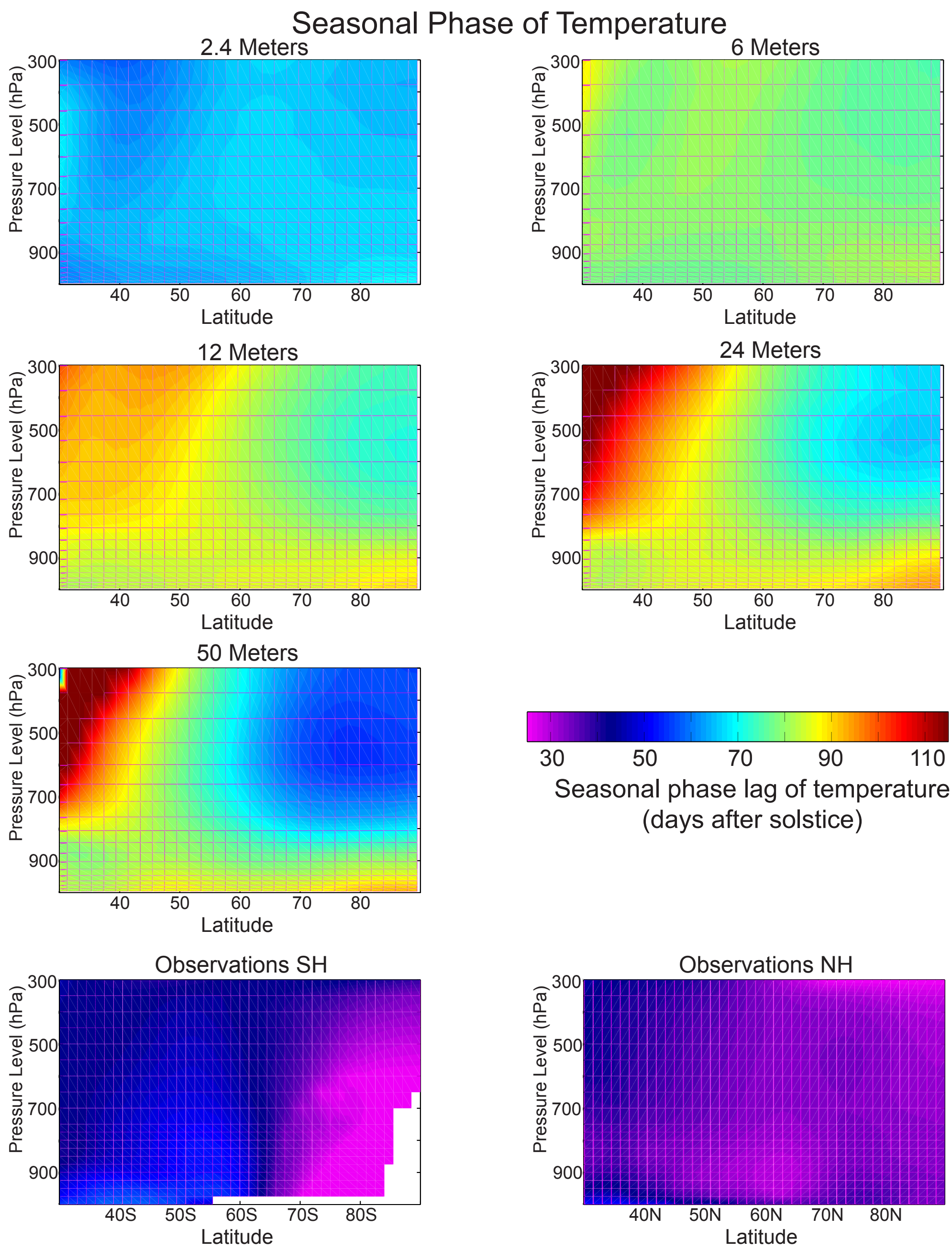

FIG. 2. Meridional-height cross sections of the phase of the seasonal cycle of atmospheric temperature in each of the slab-ocean aquaplanet simulations (upper panels) and the observations (lower panels). Values are expressed as the phase lag relative to the insolation.

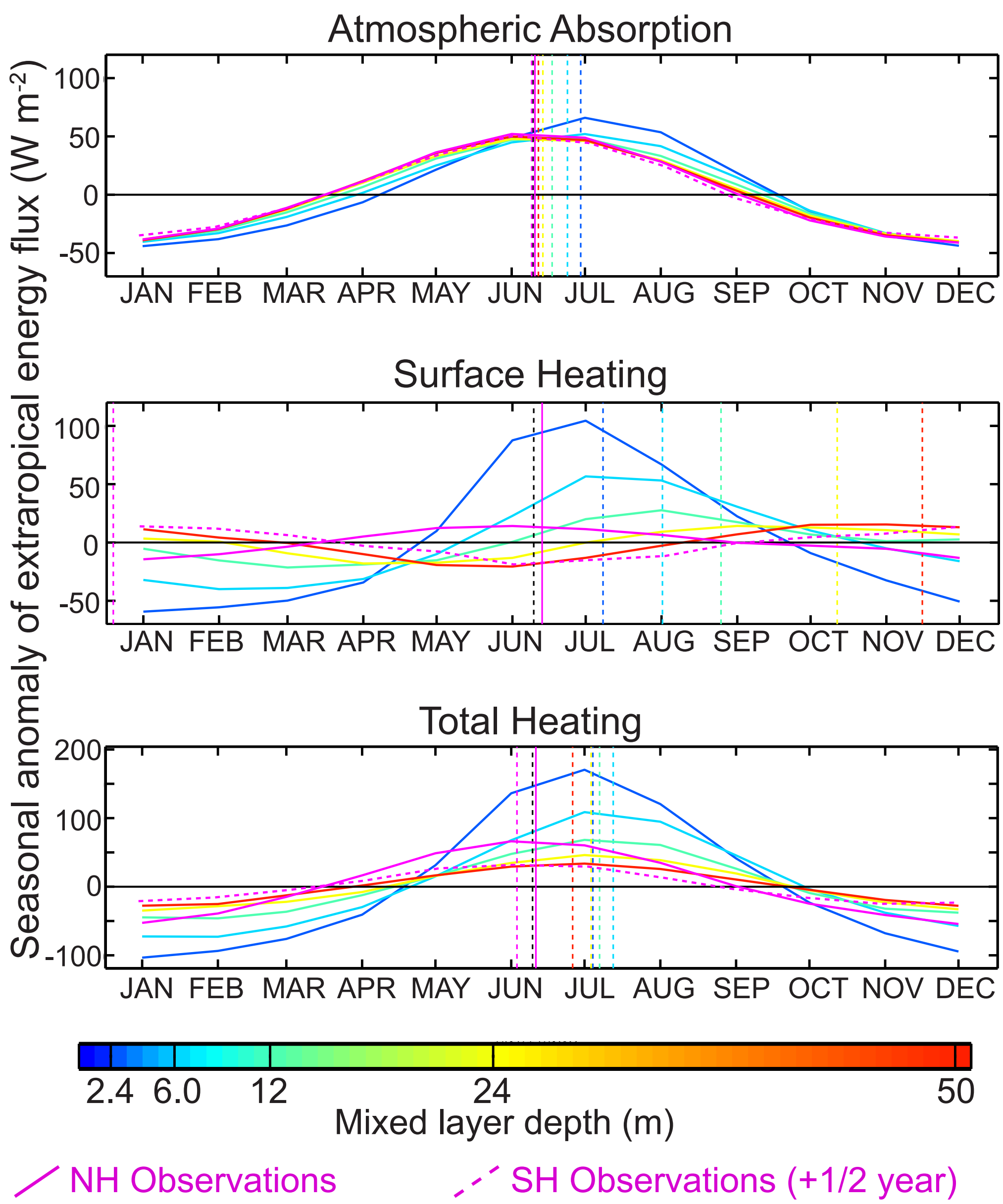

FIG. 3. Time series of atmospheric heating averaged over the Northern Extratropics defined as poleward of 40°N. The total atmospheric heating (bottom panel) is decomposed into contributions from solar absorption in the atmospheric column (top) and surface energy fluxes (middle panel). The annual mean value of each contribution has been subtracted from the time series. The different ocean mixed layer depths are indicated by the color in the colorbar at the bottom and the observations in the Northern and Southern hemisphere are shown by the solid and dashed purple lines respectively. The SH curve has been shifted by half a year. The dashed solid lines represnt the phase of the seasonal cycle and the solid black line is the summer solstice.

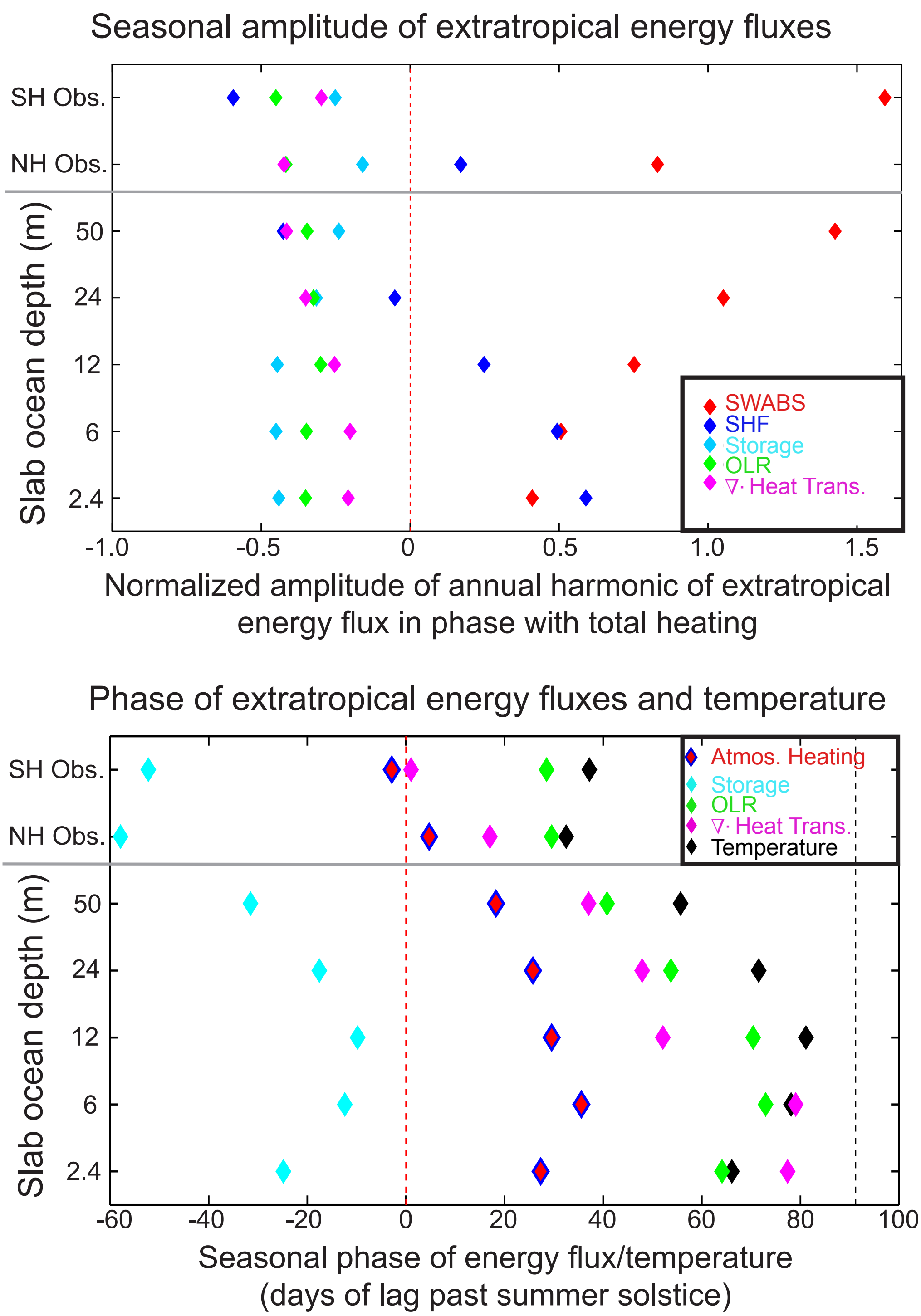

FIG. 4. (Top Panel) The normalized seasonal amplitude of energy fluxes to the extratropics, defined as the amplitude of the annual harmonic in phase with the total atmospheric heating (*SWABS* + *SHF*). The amplitude is normalized by the amplitude of the total heating to demonstrate the relative amplitude of the terms in the different mixed layer depth experiments. (Bottom Panel) The phase of the various energy flux terms in the extratropics. The temperature is the atmospheric column integrated temperature. The red and black dashed vertical lines represent the solstice and equinox respectively.